一般社団法人 電子情報通信学会
THE INSTITUTE OF ELECTRONICS,
INFORMATION AND COMMUNICATION ENGINEERS

信学技報
IEICE Technical Report

Time-Domain Selective Mapping Technique for Filtered SC-FDE

Amnart BOONKAJAY † and Fumiyuki ADACHI ‡

† ‡ Department of Communications Engineering, Graduate School of Engineering, Tohoku University
6-6-05 Aza-Aoba, Aramaki, Aoba-ku, Sendai, Miyagi, 980-8579 Japan
E-mail: † amnart@mobile.ecei.tohoku.ac.jp ‡ adachi@ecei.tohoku.ac.jp

Abstract Transmit filtering, transmit equalization, precoding, or power allocation possibly increases the peak-to-average power ratio (PAPR) of transmit single-carrier (SC) signal due to change in frequency-domain spectrum. Recently, we proposed a frequency-domain based selective mapping (FD-SLM) for suppressing the increased PAPR introduced by the transmit frequency-domain equalization (Tx-FDE). However, FD-SLM provides minor contribution when computational complexity is considered. Motivated by the fact that a "bad" arrangement of modulated symbols in a transmission block leads to high peak power, we introduce phase rotation in time domain. In this paper, we propose a time-domain phase rotation called time-domain SLM (TD-SLM). PAPR and BER performances when using the proposed TD-SLM are evaluated by computer simulation and are compared to conventional square-root Nyquist filtered SC-FDE, joint Tx/Rx SC-FDE, and those transmission schemes with FD-SLM.

Keyword Single-carrier (SC) transmission, peak-to-average power ratio (PAPR), selective mapping (SLM), frequency-domain equalization (FDE)

1. Introduction

Broadband wireless channel is characterized as a frequency-selective fading channel, in which inter-symbol interference (ISI) degrades the bit-error rate (BER) performance [1]. Multi-carrier transmission e.g. orthogonal frequency division multiplexing (OFDM) is robust against fading, but its high peak-to-average power ratio (PAPR) is the main drawback [2]. On the other hand, single-carrier (SC) transmission [3] is more attractive for uplink transmissions, e.g., in LTE-Advanced (LTE-A) system, because of lower PAPR, while the use of frequency-domain equalization (FDE) can take advantage of channel frequency selectivity to improve the BER performance [4].

SC signal can be generated by inserting discrete Fourier transform (DFT) into conventional OFDM transmitter [5], providing flexibility of signal manipulations in frequency domain, e.g., mapping, filtering, and precoding. Minimum mean-square error based joint transmit/receive FDE (joint Tx/Rx MMSE-FDE) [6] is a low-complexity SC transmission technique, where transmit FDE (Tx-FDE) receive FDE (Rx-FDE) are jointly optimized. Even though joint Tx/Rx SC-FDE provides better BER performance compared to conventional SC-FDE, it increases the PAPR because of changes in spectrum shape, implying that PAPR reduction algorithm is necessary.

We recently proposed a frequency-domain based selective mapping (FD-SLM) technique for SC-FDE and joint Tx/Rx SC-FDE [7]. Signal candidates for selection are generated by applying phase rotation to frequency-domain signal prior to inverse fast Fourier transform (IFFT). FD-SLM provides up to 2 dB PAPR reduction for joint Tx/Rx SC-FDE. However, a contribution of PAPR reduction is minor when computational complexity is considered [8]. Note that the PAPR performance of FD-SLM on square-root Nyquist filtered SC-FDE has not been yet examined [9].

The peak power of time-domain SC-FDE waveform depends on the combination of data symbols in a block. A "bad" combination of data symbols in a transmission block possibly leads to high peak power [10, 11]. This motivates us to generate candidates for SLM by applying phase rotation in time domain instead of in frequency domain.

Therefore, in this paper, we propose a time-domain based SLM (TD-SLM) for square-root Nyquist SC-FDE and joint Tx/Rx SC-FDE. Phase rotation is applied to the time-domain transmit block before transmit filtering or Tx-FDE. PAPR and BER performances when using the proposed TD-SLM are evaluated by computer simulation and are compared to conventional square-root Nyquist filtered SC-FDE, joint Tx/Rx SC-FDE, and those with FD-SLM. It should be noted that Tx-FDE and Rx-FDE weights in [6] can be used with TD-SLM without modification and no BER performance degradation is produced as far as phase rotation is perfectly known at the receiver ($\log_2 U$-bit side information needs to be transmitted to the receiver side, where U is number of candidates).

The remaining of this paper is organized as follows. Section 2 proposes TD-SLM. The transceiver model is described for square-root Nyquist filtered SC-FDE using TD-SLM in Section 3 and for joint Tx/Rx SC-FDE using TD-SLM in Section 4. Section 5 provides performance evaluation, and Section 6 concludes the paper.

2. TD-SLM algorithm

SLM [7] has been introduced as a frequency-domain based PAPR reduction technique with relatively small

This article is a technical report without peer review, and its polished and/or extended version may be published elsewhere.
Copyright ©2013 by IEICE

overhead and without distortion on waveform. In this paper, we introduce a new SLM technique which the phase rotation is applied in time-domain, called TD-SLM.

PAPR of the time-domain transmit signal calculated over a transmission block with oversampling is expressed by.

$$PAPR(\mathbf{s}) = \frac{\max\left\{\left|s(n)\right|^2\right\}}{E[\left|s(n)\right|^2]}, n = 0, \frac{1}{V}, \frac{2}{V}, ..., N_c - 1, \quad (1)$$

where V is oversampling factor.

A set of U different phase-rotation sequences $\mathbf{P}_u$ is defined and multiplied to the time-domain transmit block $\mathbf{d}$ in order to generate U different time-domain transmit block candidates. Note that the first candidate $\mathbf{P}_0$ is set to be all "1" sequence as a representative of original transmit block, where the other candidates are generated either in a deterministic or random approach as $P_u(n)=\pm 1$, $n=0\sim M-1$. In this paper, we assume the phase-rotation sequence to be real number in order to reduce the number of complex-valued multiplication, and unit-magnitude in order to meet the transmit power constraint. The instantaneous PAPR of time-domain transmit signal after filtering or applying Tx-FDE $\mathbf{s}_u$ for all u are calculated, and the phase-rotation sequence index $\hat{u}$, whose provides the lowest PAPR, is selected by

$$\hat{u} = \arg \min_{u=0,1,...,U-1} PAPR(\mathbf{s}_u = \mathbf{F}_{N_c}^H \mathbf{H}_T \mathbf{E}_M \mathbf{P}_u \mathbf{d}), \quad (2)$$

for square-root Nyquist filtered SC-FDE, and

$$\hat{u} = \arg \min_{u=0,1,...,U-1} PAPR(\mathbf{s}_u = \mathbf{F}_{N_c}^H \mathbf{W}_T \mathbf{F}_M \mathbf{P}_u \mathbf{d}), \quad (3)$$

for joint Tx/Rx SC-FDE. Note that each matrix and vector representation for square-root Nyquist SC-FDE and joint Tx/Rx SC-FDE will be described in more details in Section 3 and Section 4, respectively.

3. TD-SLM for square-root Nyquist filtered SC-FDE

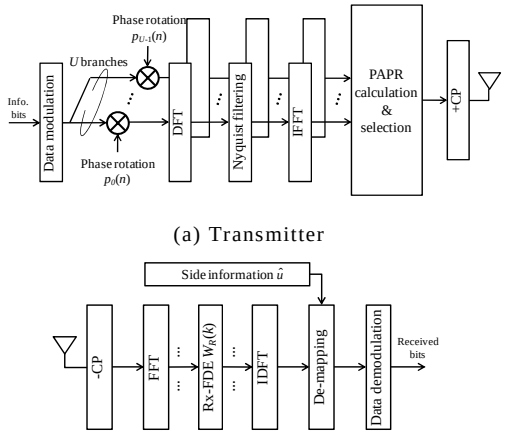

(a) Transmitter

(b) Receiver

Fig.1 Transmission system models of square-root Nyquist filtered SC-FDE with TD-SLM.

Single-user M-length block transmission over N_c subcarriers ($N_c \geq M$) with N_g-length of cyclic prefix insertion is assumed. DFT and its inverse operation are used in the transmission scheme for reaching frequency-domain processing, where filtering can be simply done as one-tap multiplication. In a system using the proposed TD-SLM, time-domain symbols are mapped by multiplying with phase-rotation sequence prior to applying DFT. Transceiver of square-root Nyquist filtered SC-FDE equipped with TD-SLM is illustrated by Fig. 1.

3.1. Transmitter

Transmitter of square-root Nyquist filtered SC-FDE equipped with TD-SLM is shown in Fig. 1(a). We begin with a block of M data-modulated symbols $\mathbf{d}=[d(0),d(1),\ldots,d(M-1)]^T$. The block $\mathbf{d}$ is used to generate U candidates for SLM $\mathbf{d}_u$ by multiplying different phase-rotation sequence. The u-th candidate block is expressed by

$$\mathbf{d}_u = \mathbf{P}_u \mathbf{d}, \quad (4)$$

where $\mathbf{P}_u \equiv diag[P_u(0),\ldots,P_u(M-1)]$ represents phase rotation matrix. The detail of phase-rotation sequence $P_u(k)$ is already discussed in Section 2.

Next, each transmit block candidate is transformed into frequency domain, and then the frequency components are copied to the entire N_c subcarrier (assuming $N_c=2M$ for simplicity). A row-repeated DFT matrix $\mathbf{E}_M$ is introduced in order to applied DFT and copying simultaneously. $\mathbf{E}_M$ is expressed by

$$\mathbf{E}_M = \begin{bmatrix} \mathbf{f}_M(\frac{M}{2}) \\ \vdots \\ \mathbf{f}_M(M-1) \\ \mathbf{f}_M(0) \\ \vdots \\ \vdots \\ \mathbf{f}_M(M-1) \\ \mathbf{f}_M(0) \\ \vdots \\ \mathbf{f}_M(\frac{M}{2}-1) \end{bmatrix}, \quad (5)$$

where $\mathbf{f}_M(m)$ is a row vector from the mth row of M-point DFT matrix $\mathbf{F}_M$, which is expressed by

$$\mathbf{F}_M = \frac{1}{\sqrt{M}} \begin{bmatrix} 1 & 1 & \cdots & 1 \\ 1 & e^{\frac{-j2\pi(1)(1)}{M}} & \cdots & e^{\frac{-j2\pi(1)(M-1)}{M}} \\ \vdots & \vdots & \ddots & \vdots \\ 1 & e^{\frac{-j2\pi(M-1)(1)}{M}} & \cdots & e^{\frac{-j2\pi(M-1)(M-1)}{M}} \end{bmatrix}, \quad (6)$$

and its Hermitian transpose $\mathbf{F}_M^H$ represents inverse operation. Frequency components of the u-th candidate $\mathbf{D}_u=[D_u(0),D_u(1),\ldots,D_u(N_c-1)]^T$ is obtained from $\mathbf{D}_u=\mathbf{E}_M\mathbf{d}_u$. After that, transmit filtering is applied to frequency

components of the u-th candidate by multiplying with transmit filtering matrix $\mathbf{H}_T$. $\mathbf{H}_T$ is a $N_c \times N_c$ diagonal matrix with J central elements in the diagonal represent filter coefficients and is expressed by

$$\mathbf{H}_T = diag\left[0,...,H_T(\frac{N_c - J}{2}),...,H_T(\frac{N_c + J}{2} - 1),...,0\right] \quad (7)$$

Here, $J=(1+\alpha)M$ where α is filter roll-off factor. In case of transmission using square-root raised cosine (SRRC) filter [9], the filter coefficients $H_T(k)$ can be determined by

$$H_T(k) = \begin{cases} 1, & 0 \le |k-M| < \frac{1-\alpha}{2}M \\ \cos[\frac{\pi}{2\alpha M}(|k| - \frac{1-\alpha}{2}M)], & \frac{1-\alpha}{2}M \le |k-M| < \frac{1+\alpha}{2}M \\ 0, & otherwise \end{cases}. \quad (8)$$

After that, the filtered signal is transformed back into time domain by N_c-point IFFT matrix $\mathbf{F}_{N_c}^H$. TD-SLM algorithm is applied in order to select the time-domain transmit signal $\mathbf{s}_{\hat{u}} = [s_{\hat{u}}(0), s_{\hat{u}}(1), \ldots, s_{\hat{u}}(N_c - 1)]^T$ as a candidate with the lowest PAPR. The time-domain transmit signal $\mathbf{s}_{\hat{u}}$ is expressed by

$$\mathbf{s}_{\hat{u}} = \mathbf{F}_{N_c}^H \mathbf{H}_T \mathbf{E}_M \mathbf{d}_{\hat{u}} = \mathbf{F}_{N_c}^H \mathbf{H}_T \mathbf{E}_M \mathbf{P}_{\hat{u}} \mathbf{d}, \quad (9)$$

where the selection of $\mathbf{s}_{\hat{u}}$ is already discussed in details in Section 2.

Finally, the last N_g samples of transmit block are copied as a cyclic prefix (CP) and inserted into the guard interval (GI), then a CP-inserted signal block of N_g+N_c samples is transmitted.

3.2. Received Signal

The propagation channel is assumed to be a symbol-space L-path frequency-selective block fading channel [1], where its impulse response between transmitter and receiver is

$$h(\tau) = \sum_{l=0}^{L-1} h_l \delta(\tau - \tau_l), \quad (10)$$

where h_l and τ_l are complex-valued path gain and time delay of the l-th path, respectively. $\delta(\cdot)$ is the delta function. Time-domain received signal after CP removal, $\mathbf{r}_{\hat{u}} = [r_{\hat{u}}(0), r_{\hat{u}}(1), ..., r_{\hat{u}}(N_c - 1)]^T$, is expressed by

$$\mathbf{r}_{\hat{u}} = \sqrt{\frac{2E_s}{T_s}} \mathbf{h} \mathbf{s}_{\hat{u}} + \mathbf{n}, \quad (11)$$

where $\mathbf{s}_{\hat{u}} = \mathbf{F}_{N_c}^H \mathbf{H}_T \mathbf{E}_M \mathbf{P}_{\hat{u}} \mathbf{d}$ is obtained from (9), and $\mathbf{n}$ is noise vector in which element is zero-mean additive white Gaussian noise (AWGN) having the variance $2N_0/T_s$ with T_s is symbol duration and N_0 being the one-sided noise power spectrum density. Channel response matrix $\mathbf{h}$ is a circular matrix representing time-domain channel response between user u and the base station, which is

$$\mathbf{h} = \begin{bmatrix} h_0 & & & h_{L-1} & \cdots & h_1 \\ h_1 & \ddots & & & \ddots & \vdots \\ \vdots & & h_0 & \mathbf{0} & & h_{L-1} \\ h_{L-1} & & h_1 & \ddots & & \\ & \ddots & \vdots & & \ddots & \\ \mathbf{0} & & h_{L-1} & \cdots & \cdots & h_0 \end{bmatrix}. \quad (12)$$

The received signal vector $\mathbf{r}_{\hat{u}}$ is transformed into frequency domain by N_c-point FFT, obtaining the frequency-domain received signal $\mathbf{R}_{\hat{u}}$ as

$$\begin{aligned} \mathbf{R}_{\hat{u}} &= \sqrt{\frac{2E_s}{T_s}} \mathbf{F}_{N_c} \mathbf{h} \mathbf{s}_{\hat{u}} + \mathbf{F}_{N_c} \mathbf{n} \\ &= \sqrt{\frac{2E_s}{T_s}} \mathbf{F}_{N_c} \mathbf{h} \mathbf{F}_{N_c}^H \mathbf{H}_T \mathbf{D}_{\hat{u}} + \mathbf{F}_{N_c} \mathbf{n}, \\ &= \sqrt{\frac{2E_s}{T_s}} \mathbf{H}_c \mathbf{H}_T \mathbf{D}_{\hat{u}} + \mathbf{N} \end{aligned} \quad (13)$$

where the frequency-domain channel response $\mathbf{H}_c$ is

$$\mathbf{F}_{N_c} \mathbf{h} \mathbf{F}_{N_c}^H = diag[H_c(0),...,H_c(N_c - 1)] \equiv \mathbf{H}_c. \quad (14)$$

In this paper, we introduce joint MMSE-FDE and spectrum combining instead of conventional M-point MMSE-FDE in order to utilize the excess-bandwidth frequency components and achieve additional frequency diversity gain [12]. FDE matrix $\mathbf{W}$ with a dimension of $M \times N_c$ is expressed by

$$\mathbf{W} = \begin{bmatrix} & & W(\frac{N_c}{4}) & & & W(\frac{3N_c}{4} - 1) & \\ & \mathbf{0} & & & & & \ddots \\ & & & & & & W(N_c - 1) \\ W(0) & & & \ddots & & & \\ & \ddots & & & & \mathbf{0} & \\ & & W(\frac{N_c}{4} - 1) & & W(\frac{3N_c}{4} - 1) & & \end{bmatrix}, \quad (15)$$

where $W(k)$, $k=0 \sim N_c - 1$ is determined so as to minimize the mean-square error (MSE) between $\mathbf{D}_{\hat{u}}$ and the frequency-domain signal after equalization $\hat{\mathbf{D}}_{\hat{u}} = \mathbf{W}\mathbf{R}_{\hat{u}}$, and given by

$$W(k) = \frac{H_c^*(k) H_T^*(k)}{\sum_{g=0}^{1} |H_c(k \bmod M + gM) H_T(k \bmod M + gM)|^2 + \left(\frac{E_s}{N_0}\right)^{-1}}. \quad (16)$$

where $H_c(k)$ is the elements in $\mathbf{H}_c$ with respect to each frequency index.

The frequency-domain received signal after equalization and spectrum combining $\hat{\mathbf{D}}_{\hat{u}}$ is finally transformed back into time-domain by M-point inverse DFT (IDFT). Therefore, the time-domain received signal before de-mapping $\hat{\mathbf{d}}_{\hat{u}} = [\hat{d}_{\hat{u}}(0), \hat{d}_{\hat{u}}(1), \ldots, \hat{d}_{\hat{u}}(M-1)]^T$ is

$$\hat{\mathbf{d}}_{\hat{u}} = \mathbf{F}_M^H \hat{\mathbf{D}}_{\hat{u}} = \mathbf{F}_M^H \mathbf{W} \mathbf{R}_{\hat{u}} + \mathbf{F}_M^H \mathbf{W} \mathbf{N}. \quad (17)$$

De-mapping is applied to time-domain signal after FDE and spectrum combining in order to obtain the original time-domain transmission block. De-mapping is simply done by multiplying $\hat{\mathbf{d}}_{\hat{u}}$ with the Hermitian transpose of

selected phase-rotation sequence, obtaining time-domain received vector $\hat{\mathbf{d}}=[\hat{d}(0),\hat{d}(1),\ldots,\hat{d}(M-1)]^T$ as

$$\hat{\mathbf{d}}=\mathbf{P}_{\hat{u}}^H\hat{\mathbf{D}}_{\hat{u}}. \quad (18)$$

From (18), it is observed that the receiver needs to know which phase-rotation sequence is selected as a sequence providing the lowest PAPR; otherwise an accurate de-mapping cannot be achieved. This implies that up to $\log_2 U$ bits of explicit side information is mandatory (as shown in Fig. 1(b)).

4. TD-SLM for joint Tx/Rx SC-FDE

Transceiver model of joint Tx/Rx SC-FDE and TD-SLM is illustrated by Fig. 2, where the Nyquist filtering is replaced by Tx-FDE weight compared to square-root Nyquist filtered SC-FDE. Similar to Fig. 1, phase rotation is employed before DFT.

4.1 Transmitter

M-length of block transmission over N_c subcarriers is considered in this section, however, excess-bandwidth transmission with roll-off factor α is not considered. Similar to Section 2, a transmission block consisting of M data-modulated symbols $\mathbf{d}=[d(0),d(1),\ldots,d(M-1)]^T$ is used to generate U candidates for SLM $\mathbf{d}_u$ by multiplying different phase-rotation sequence, then each transmission block candidate is transformed into frequency domain by M-point DFT, yielding frequency components of the u-th candidate $\mathbf{D}_u=[D_u(0),D_u(1),\ldots,D_u(N_c-1)]^T$ as

$$\mathbf{D}_u=\mathbf{F}_M\mathbf{P}_u\mathbf{d}. \quad (19)$$

Next, $\mathbf{D}_u$ is multiplied by Tx-FDE weight matrix, represented by a $N_c\times N_c$ diagonal matrix $\mathbf{W}_T=diag[W_T(0),\ldots,W_T(M-1),0,\ldots,0]$, obtaining the frequency component after applying Tx-FDE of the u-th candidate $\mathbf{S}_u=\mathbf{W}_T\mathbf{D}_u$. Note that Tx-FDE weight calculation is described in Subsection 3.3.

After that, $\mathbf{S}_u$ is transformed back into time domain by N_c-point IFFT matrix $\mathbf{F}_{N_c}^H$. TD-SLM algorithm is applied in order to select the time-domain transmit signal $\mathbf{s}_{\hat{u}}=[s_{\hat{u}}(0),s_{\hat{u}}(1),\ldots,s_{\hat{u}}(N_c-1)]^T$ as a candidate with the lowest PAPR. The time-domain transmit signal $\mathbf{s}_{\hat{u}}$ is expressed by

$$\mathbf{s}_{\hat{u}}=\mathbf{F}_{N_c}^H\mathbf{W}_T\mathbf{F}_M\mathbf{d}_{\hat{u}}=\mathbf{F}_{N_c}^H\mathbf{W}_T\mathbf{F}_M\mathbf{P}_{\hat{u}}\mathbf{d}. \quad (20)$$

4.2 Receiver

The propagation channel in this section is exactly the same as in Section 2. It is also observed that the receiver model is Fig. 2(b) is similar to Fig. 1(b), except joint MMSE-FDE and spectrum combining is replaced by Rx-FDE. The frequency-domain received signal $\mathbf{R}_{\hat{u}}$ is expressed by

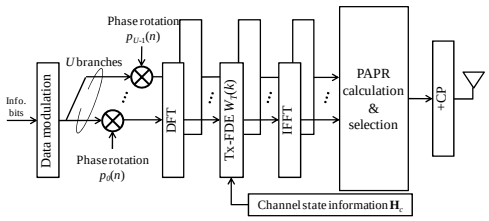

(a) Transmitter

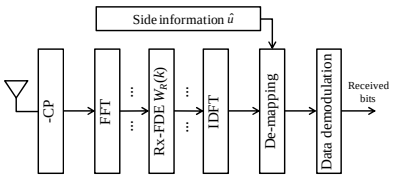

(b) Receiver

Fig.2 Transmission system models of joint Tx/Rx SC-FDE with TD-SLM.

$$\begin{aligned}\mathbf{R}_{\hat{u}} &= \sqrt{\frac{2E_s}{T_s}}\mathbf{F}_{N_c}\mathbf{h}\mathbf{F}_{N_c}^H\mathbf{W}_T\mathbf{D}_{\hat{u}}+\mathbf{F}_{N_c}\mathbf{n}\\ &= \sqrt{\frac{2E_s}{T_s}}\mathbf{H}_c\mathbf{W}_T\mathbf{D}_{\hat{u}}+\mathbf{N}\end{aligned}. \quad (21)$$

Rx-FDE $\mathbf{W}_R=diag[W_R(0),\ldots,W_R(N_c-1)]$ is applied at the receiver as a joint cooperation with Tx-FDE to reduce the effect from frequency-selective fading. The received signal after equalization $\hat{\mathbf{D}}_{\hat{u}}=\mathbf{W}_R\mathbf{R}_{\hat{u}}$, where $\hat{\mathbf{D}}_{\hat{u}}=[\hat{D}_{\hat{u}}(0),\hat{D}_{\hat{u}}(1),\ldots,\hat{D}_{\hat{u}}(M-1)]^T$, is later transformed back into time domain by M-point IDFT, yielding time-domain signal before de-mapping $\hat{\mathbf{d}}_{\hat{u}}=[\hat{d}_{\hat{u}}(0),\hat{d}_{\hat{u}}(1),\ldots,\hat{d}_{\hat{u}}(M-1)]^T$ as

$$\hat{\mathbf{d}}_{\hat{u}}=\mathbf{F}_M^H\hat{\mathbf{D}}_{\hat{u}}=\mathbf{F}_M^H\mathbf{W}_R\mathbf{R}_{\hat{u}}+\mathbf{F}_M^H\mathbf{W}_R\mathbf{N}. \quad (22)$$

Note that the dimension of $\hat{\mathbf{D}}_{\hat{u}}$ is reduced to be $M\times 1$ since $\hat{D}_{\hat{u}}(k)=0$ for $k=M\sim N_c-1$.

Finally, de-mapping is applied as the same as in Subsection 2.2, resulting in time-domain received vector $\hat{\mathbf{d}}=[\hat{d}(0),\hat{d}(1),\ldots,\hat{d}(M-1)]^T$ as

$$\hat{\mathbf{d}}=\mathbf{P}_{\hat{u}}^H\hat{\mathbf{D}}_{\hat{u}}. \quad (23)$$

4.3 FDE weights calculation

Performance of joint Tx/Rx SC-FDE in aspect of BER performance has been exhaustively discussed in [6]. In this subsection, we expect to use the proposed FDE weights in [6] without modifications even though TD-SLM is employed.

Joint FDE weights calculation begins from the receiver. By using the MMSE criterion where the MSE is calculated between frequency-domain transmitted and received signal, an error vector $\mathbf{e}$ is given by

$$\mathbf{e}=\hat{\mathbf{D}}_{\hat{u}}-\sqrt{\frac{2E_s}{T_s}}\mathbf{D}_{\hat{u}}=\sqrt{\frac{2E_s}{T_s}}(\mathbf{W}_R\mathbf{H}_c\mathbf{W}_T-\mathbf{I}_M)\mathbf{D}_{\hat{u}}+\mathbf{W}_R\mathbf{N}. \quad (24)$$

From (24), it can be observed that the error vector and the MSE function $e=tr[E(\mathbf{e}\mathbf{e}^H)]$ are independent from phase-rotation sequence since $tr[E(\mathbf{D}_u\mathbf{D}_u^H)]=1$ for all

u=0~U-1. This clarifies that the original FDE weights in [6] can be used with TD-SLM without modifications. Therefore, $W_R(k)$ and $W_T(k)$ can be expressed as follows.

$$W_R(k) = \frac{H_c^*(k)W_T^*(k)}{\left|H_c(k)W_T(k)\right|^2 + \left(E_s/N_0\right)^{-1}}. \quad (25)$$

$$W_T(k) = \max\left[\left\{\sqrt{\frac{(E_s/N_0)^{-1/2}}{\sqrt{\kappa}\left|H_c(k)\right|}} - \frac{(E_s/N_0)^{-1}}{\left|H_c(k)\right|^2}\right\}, 0\right]. \quad (26)$$

Note that κ is a parameter selected to satisfy the transmit power constraint $(1/N_c)\sum_{k=0}^{N_c-1}\left|W_T(k)\right|^2 = 1$. It is also observed the transmitter requires channel information.

5. Performance Evaluation

Numerical and simulation parameters are summarized in Table 1. We assume 16-QAM block transmission with the number of available subcarriers N_c=128. System performance is evaluated in terms of PAPR, BER, and computational complexity.

Table 1 Simulation parameters.

Transmitter	Data modulation	SC-16QAM
	# of symbols per block	M = 64
	FFT/IFFT block size	N_c = 128
	Cyclic prefix length	N_g = 16
	Average transmit E_b/N_0	10 dB
	Transmit filtering	SRRC (α = 0~1), Tx-FDE
SLM parameters	Phase-rotation sequence type	4095-bit long PN
	# of candidates	U = 1(no SLM)~64
	Oversampling factor	V = 8
Channel	Fading	Frequency-selective block Rayleigh
	Power delay profile	Symbol-spaced 16-path uniform
Receiver	Channel estimation	Ideal
	Side information	Ideal

5.1 PAPR performance

PAPR performance is evaluated by examining the complementary cumulative distribution function (CCDF). Fig. 3 shows the comparison of PAPR performance of conventional square-root Nyquist filtered SC-FDE, square-root Nyquist filtered SC-FDE with FD-SLM [7], and with the proposed TD-SLM, at roll-off factor α=0 and 0.5. It can be observed that up to 2.12 dB and 0.1 dB of 99.9% outage PAPR reduction from conventional SC-FDE are achieved for transmission using FD-SLM with U=64 at α=0 and 0.5, respectively. On the other hand, TD-SLM outperforms FD-SLM by achieving 3 dB and 0.8 dB of 99.9% outage PAPR reduction from conventional SC-FDE with U=64 at α=0 and 0.5, respectively. This is consistent with our motivation as generating candidates for SLM in time domain is better than in frequency domain, since bad arrangement of transmit symbol blocks is eliminated. However, it is also observed that SLM provides a small contribution when α increases in FD-SLM. This is because the frequency components at the edges of spectrum are suppressed by filter coefficients when α increases, resulting in smaller effect on peak power when the frequency components are rotated.

Fig. 4 shows the comparison of PAPR performance of conventional joint Tx/Rx SC-FDE, joint Tx/Rx SC-FDE with FD-SLM [7], and with the proposed TD-SLM. It can be seen that TD-SLM outperforms FD-SLM in every number of candidates U. However, it is also observed that performance gap between TD-SLM and FD-SLM is narrow when U increases, especially when U=64. This can be described as change in spectrum shape occurred by Tx-FDE is more severe even though a good arrangement of transmit symbols block is selected before applying Tx-FDE in frequency domain.

Table 2 Computational complexity.

	No-SLM	**FD-SLM[7]**	**TD-SLM**
Phase rotation			
DFT (or FFT)	$M\log_2(M)$	$M\log_2(M)$	$U\times M\log_2(M)$
Tx-FDE weight calculation	$2M$	$2M$	$2M$
IFFT	$N_c\log_2(N_c)$	$U\times(VM)\log_2(VM)$	$U\times(VM)\log_2(VM)$
PAPR calculation		$U\times(VM)$	$U\times(VM)$

5.2 BER performance

Fig. 5 shows the BER as a function of average received bit energy-to-noise power spectrum density ratio $E_b/N_0=0.25(E_s/N_0)(1+N_g/N_c)$. Fig. 5 confirms that the BER performances of square-root Nyquist filtered SC-FDE at α=0 and 0.5, and joint Tx/Rx SC-FDE when TD-SLM is employed are the same as transmission without SLM as far as perfect side information is achieved. BER performance of square-root Nyquist filtered SC-FDE at α=0.5 is better than α=0.5 due to additional frequency diversity, however, the transmission bandwidth increases by a factor of 1+α. In addition, joint Tx/Rx SC-FDE provides the best BER performance among these transmission schemes as a contribution from ISI reduction.

5.3 Computational complexity

In this paper, computational complexity is evaluated by computing the number of complex-valued multiplications [8]. As indicated in [7], SLM requires high computational complexity due to an increasing of IFFT operation.

Table 2 shows the computational complexity of transmitters of conventional SC-FDE, SC-FDE with FD-SLM, and TD-SLM. It is observed that TD-SLM has more computational complexity since it requires U times of DFT operation. However, DFT can be replaced by FFT if the number of symbols per block is expressed in term of

2^n. Complexity from FFT operation is relatively small since oversampling is not considered. For example, assuming M=64, U=64, and V=8, the additional complexity of TD-SLM compared to FD-SLM is only 10%. This summarizes that the proposed TD-SLM provides better PAPR performance without performance degradation on BER, and with a small additional complexity compared to FD-SLM in [7].

6. Conclusion

In this paper, we proposed the TD-SLM for broadband square-root Nyquist filtered SC-FDE and joint Tx/Rx SC-FDE. The proposed TD-SLM generates transmit block candidates in time domain prior to DFT. It is confirmed in the paper that conventional Tx-FDE and Rx-FDE weights can be employed without modifications when TD-SLM is applied. Simulation results confirmed that the better PAPR performance is achieved without BER degradation compared to FD-SLM.

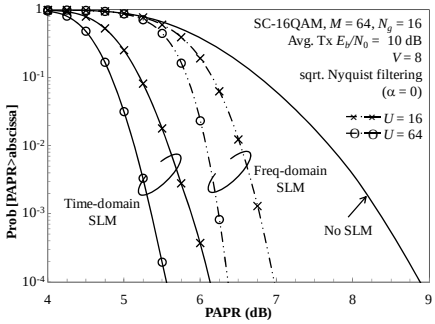

(a) α=0

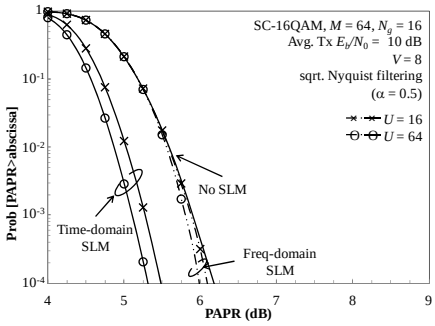

(b) α=0.5

Fig.3 CCDF of PAPR of square-root Nyquist filtered SC-FDE.

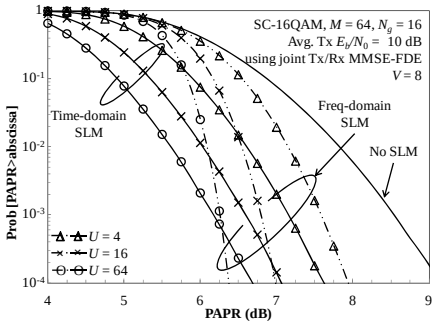

Fig.4 CCDF of PAPR of joint Tx/Rx SC-FDE.

References

[1] A. Goldsmith, *Wireless Communications*, Cambridge University Press, 2005.

[2] S. H. Han and J. H. Lee, "An Overview of Peak-to-Average Power ratio Reduction Techniques for Multicarrier Transmission," *Wireless Communications, IEEE*, vol. 12, no. 2, pp. 56-65, April 2005.

[3] H. Sari, G. Karam, and I. Jeanclaude, "Transmission Techniques for Digital Terrestrial TV Broadcasting," *IEEE Commun. Mag.*, vol. 33, pp. 100-109, February 1995.

[4] D. Falconer, S. Ariyavisitakul, A. Benyamin-Seeyar, and B. Eidson, "Frequency Domain Equalization for Single-Carrier Broadband Wireless Systems," *Communications Magazine, IEEE*, vol. 40, no. 4, pp. 58-66, April 2002.

[5] H. Wu, and T. Haustein, "Radio Resource Management for the Multi-User Uplink Using DFT-Precoded OFDM," *in Proc. IEEE International Conference on Communications (ICC 2008)*, May 2008.

[6] K. Takeda, and F. Adachi, "Joint Iterative Transmit/Receive FDE&FDIC for Single-Carrier Block Transmissions," *IEICE Trans. Commun.*, vol. E94-B, no. 5, pp. 1396-1404, May 2011.

[7] A. Boonkajay, T. Obara, T. Yamamoto, and F. Adachi, "Selective Mapping for Broadband Single-Carrier Transmission Using Joint Tx/Rx MMSE-FDE," *in Proc. IEEE 24th International Symposium on Personal Indoor and Mobile Radio Communications (PIMRC 2013)*, Sept. 2013.

[8] K. Tenma, T. Yamamoto, K. Lee, and F. Adachi, "2-step QRM-MLBD for Broadband Single-carrier Transmission," *IEICE Trans. Commun.*, vol. E95-B, no. 4, pp. 1366-1374, April 2012.

[9] Y. Akaiwa, *Introduction to Digital Mobile Communication*, 1st ed., Wiley, 1997.

[10] Dov Wulich and Lev Goldfield, "Bound of the Distribution of Instantaneous Power in Single Carrier Modulation," *IEEE Trans. Wireless Commun.*, vol. 4, no. 4, pp. 1773-1778, July 2005.

[11] Vincent K. N. Lau, "Average of Peak-to-Average Ratio (PAR) of IS95 and CDMA2000 Systems – Single Carrier," *IEEE Commun. Lett.*, vol. 5, no. 4, pp. 160-162, April 2001.

[12] T. Obara, K. Takeda, and F. Adachi, "Joint Frequency-Domain Equalization and Spectrum Combining for the Reception of SC Signals in the Presence of Timing Offset," *in Proc. IEEE 71st Vehicular Technology Conference (VTC-Spring)*, May 2010.

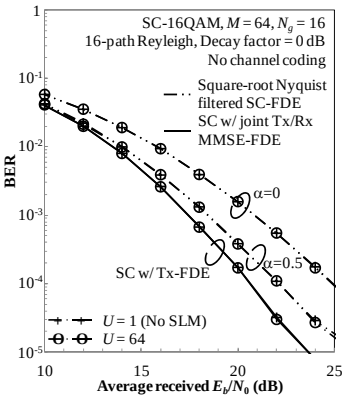

Fig.5 BER performance.